New results on T–S fuzzy sampled-data stabilization for switched chaotic systems with its applications

R. Vadivel [a], S. Sabarathinam [b], Yongbao Wu [c,d,*], Kantapon Chaisena [a],
Nallappan Gunasekaran [e,*]

[a] *Department of Mathematics, Phuket Rajabhat University, Phuket 83000, Thailand*
[b] *Laboratory of Complex Systems Modeling and Control, National Research University, High School of Economics, Moscow, Russia*
[c] *School of Automation, Southeast University, Nanjing 210096, China*
[d] *School of Mathematical and Computational Science, Hunan University of Science and Technology, Xiangtan 411201, China*
[e] *Computational Intelligence Laboratory, Toyota Technological Institute, Nagoya, 468-8511, Japan*

ARTICLE INFO

ABSTRACT

This study presents a T–S fuzzy-based sampled-data controller for switched chaotic systems. First, we designed the switched-based sampled-data fuzzy controller. Second, a novel time-dependent Lyapunov–Krasovskii functional (LKF) approach with the information of switching signals is proposed, which covers all information of the sampling interval and the time-delay information in the controller, improving the integral inequality, some sufficient conditions are established, which makes the proposed closed-loop system be exponentially stable. Subsequently, the derived conditions are formulated with respect to linear matrix inequalities (LMIs). Meanwhile, the corresponding sampled-data controller gains are designed under the larger sampling interval. Finally, the suggested T–S fuzzy sampled-data controller (TSFSD) is used to demonstrate the usefulness of the approaches in the Lorenz system, Chen system, and Lu system.

1. Introduction

Lotfi A. Zadeh's fuzzy logic theory has revolutionized current science and technology research and development. In control theory, fuzzy logic has been crucial. It has provided fresh logical insights [1]. The Takagi–Sugeno (T–S) fuzzy model is mathematically straightforward. It has become one of the most widely used tools for the design and analysis of control systems [2,3]. Nonlinear control methods based on the T–S fuzzy model have recently been developed effectively in the context of linear matrix inequalities (LMIs) (see [4–8]). The T–S fuzzy model approach was widely used in the description of actual systems as a great way for dealing with system intrinsic parameter insecurity in [9–13]. In [14], the control of T–S fuzzy systems with engineering-oriented complexity was explored by the authors. Accordingly, some of the control methods have been developed for fuzzy-based nonlinear systems.

Recently, the chaotic system has been an essential one that has drawn a lot of attention from both academic and industrial groups. In this regard, chaotic systems have numerous potential uses in the engineering field, including secure communication, neural networks, and etc [15–18]. In [19], initiated the master–slave concept was initiated

to fulfill the synchronization of chaotic systems. Up to now, different control approaches have been proposed to examine chaotic systems, for example, feedback control [20], intermittent control [21], sliding mode control [22], adaptive control [23], and impulsive control [24]. In [25], authors investigated reliable H_∞ control for the permanent magnet synchronous motor using fuzzy techniques. The fuzzy stabilization of nonlinear systems in sampled data in terms of exponential stability has been further developed in [26]. More recently, the authors in [27] considered fuzzy large-scale interconnected power systems of T–S and have been computing stability and stabilization issues based on the sampled-data control (SDC) approach. Recently, sampled-data feedback control is a highly examined point for finite-dimensional systems due to the way modern control systems utilize digital technology for the execution of the controller [28–31]. The control systems utilizing one or more signals at discrete time intervals are defined as SDC systems. Recently, a lot of researchers focused on the chaotic systems with SDC. The stability issue of fuzzy sampled-data stabilization of T–S for chaotic systems has been extensively investigated in [32]. The author's in [33] has been investigated chaotic systems with T–S fuzzy technique via asynchronous samplings. Although the SDC technique established a

large number of findings and produced a wider sample interval, one of the objectives of this study is to improve the sample period.

A switched system is made up of a set of continuous-time or discrete-time subsystems, as well as a switching law that determines which subsystem is active at any given time period. In the last two decades, several works have been dedicated to switched systems; see, for example, [34–37]. The sampled-data stabilization problem for switched linear neutral systems was investigated in [38]. Recently, fuzzy sampled-data stabilization for switched non-linear systems has been studied only in a few publications [39–42]. However, most methods have a similar weakness, i.e., the essential information of membership functions has been disregarded, which in some ways contributes to increased conservatively. It is observed that when the Lyapunov-reliant functional membership function is taken into consideration, the conservatism of the findings for the fuzzy systems is reduced. Consequently, the membership function in fuzzy sample data systems is highly essential and significant. Recently, the LKF, which depends on the membership function, was introduced and less conservative results were achieved in [43]. Therefore, different challenges arise. Can the subsystem constraints for switched fuzzy systems be relaxed and a sampled-data controller designed to fulfill the stay conditions? How can we ensure that the closed-loop system remains stable when asynchronous develops between an activated subsystem and its corresponding controller? These questions are answered affirmatively in this study.

The study's major goal is to solve the challenge of chaotic systems stabilizing under SDC. Novel necessary conditions for the sampled-data stabilization of chaotic systems are found utilizing the free-weighting matrix method and the LMI methodology. For chaotic systems, a novel stability criterion is developed that fully exploits the knowledge available about the actual sampling pattern. We show that under the sample-and-hold implementation of the controller, there is a tiny enough sampling time for the closed-loop system to maintain exponentially stability (Theorems 1 and 2). The simulation results are presented to illustrate the efficacy of the new approach.

Notations: We will now define a certain issue formulation and main outcome notations. $\mathbb{R}^n$ represents a n-dimensional Euclidean space, and $\mathbb{R}^{n \times m}$ represents a n-dimensional real matrix. I_n and $0_{n \times m}$ are denote $n \times n$ identity matrix and $n \times m$ zero matrix, respectively.

2. Problem statement and preliminaries

Consider a nonlinear system which can be described as the following switching signal:

$$\dot{x}(t) = f_{\sigma(t)}(x(t), u(t)), \tag{1}$$

where $x(t) \in \mathbb{R}^n$ and $u(t) \in \mathbb{R}^m$ denotes the state vector and control input, respectively. $\sigma(t) = [0, \infty) \to \mathbb{S} = \{1, \ldots, m\}$ noted right continuous piecewise constant switching signal. Furthermore, the system (1) can be described by the following fuzzy IF-THEN rules

Plant rule i: **IF** z_1 is M_{i1} and $\cdots$ and z_n is M_{in} **THEN**

$$\dot{x}(t) = A_{i\sigma(t)}x(t) + B_{i\sigma(t)}u(t), \ (i = 1, 2, \ldots, r) \tag{2}$$

where $A_{i\sigma(t)} \in \mathbb{R}^{n \times n}$, $B_{i\sigma(t)} \in \mathbb{R}^{n \times m}$, are constant system matrices, the fuzzy set noted as M_{ij} ($i = 1, \ldots, r; j = 1, \ldots, n$) and the IF-THEN rules number is r, the premise variables denoted as $z(t) = [z_1(t), \ldots, z_n(t)]$. The overall output is expressed as:

$$\dot{x}(t) = \frac{\sum_{i=1}^{r} w_i(z(t))A_{i\sigma(t)}x(t)}{\sum_{i=1}^{r} w_i(z(t))} + \frac{\sum_{i=1}^{r} w_i(z(t))B_{i\sigma(t)}u(t)}{\sum_{i=1}^{r} w_i(z(t))}.$$

Throughout this paper, we consider $\sigma(t)$ is equivalent to κ. The fuzzy model (2) is the κth subsystem and by using the standard fuzzy inference method, the given pair of $(x(t), u(t))$, the final output of the fuzzy model (2) is inferred as follows:

$$\dot{x}(t) = \sum_{i=1}^{r} h_i(z(t))[A_{i\kappa}x(t) + B_{i\kappa}u(t)], \tag{3}$$

where $h_i(z(t))$ represents the normalized weight of the IF-THEN rule,

$$h_i(z(t)) = \frac{w_i(z(t))}{\sum_{i=1}^{r} w_i(z(t))}, \ w_i(z(t)) = \prod_{j=1}^{n} M_{ij}(z_j(t))$$

and $M_{ij}(z_j(t))$ is the grade of membership of $z_j(t)$ in M_{ij}. It is assumed that $w_i(z(t)) \geq 0$, $\sum_{i=1}^{r} w_i(z(t)) > 0$. Therefore, we have $h_i(z(t)) \geq 0$, and $\sum_{i=1}^{r} h_i(z(t)) = 1$.

3. Sampled-data mechanism and PDC control law

Based on the sampled-data mechanism and parallel distributed compensation (PDC) control theory, the new fuzzy controller can be obtained as follows:

Plant rule i: **IF** $z_1(t_k)$ is M_{i1} and ... and $z_n(t_k)$ is M_{in} **THEN**

$$u(t) = u(t_k) = K_{i\sigma(t)}x(t_k), \ \text{for } t \in [t_k, \ t_{k+1}), \ i = 1, 2, \ldots, r, \tag{4}$$

where $K_{i\sigma(t)}$, $(i = 1, 2, \ldots, r)$ are the controller parameters. t_k with $k \in \mathbb{S}$ denotes the kth sampling time. Thus, the control signal has a constant value $u(t)$ for $t \in [t_k, t_{k+1})$ in which $u(t)$ denotes a control signal. The general fuzzy controller $u(t)$ is a piecewise constant and can be written as

$$u(t) = \sum_{i=1}^{r} h_i(z(t_k))K_{i\kappa}x(t_k), \tag{5}$$

for $t \in [t_k, \ t_{k+1}), \ i = 1, 2, \ldots, r.$

Set the sampling interval $h_k = t_{k+1} - t_k$ and satisfy $0 < h_{\mathcal{V}} \leq h_k \leq h_{\mathcal{U}}$, for all $k \geq 0$. Then, substituting (5) into (3), one gets

$$\dot{x}(t) = h_i h_j \left[A_{i\kappa}x(t) + (B_{i\kappa}K_{j\kappa})x(t_k) \right], \tag{6}$$

where $h_i h_j = \sum_{i=1}^{r} \sum_{j=1}^{r} h_i(z(t))h_j(z(t_k))$.

Definition 1 ([*44*]). The System (6) is said to be exponentially stable, if there exist $\alpha > 0$ and $\beta > 0$, such that the following relation is holds

$$\|x(t)\| \leq \beta e^{-\alpha(t-t_0)}\|x(t_0)\|_c, \forall t \geq t_0, \tag{7}$$

where α is the exponential delay rate and $x(t_0)$ is the initial value at $t = t_0$.

Definition 2 ([*44*]). Given constant $\tau_d > 0$, for any time interval between two successive switches is in any event τ_d, i.e. $t_{s+1}^\sigma - t_s^\sigma > \tau_d$. If there exists $N_0 > 0$ such that

$$N_\sigma(T, t) \leq N_0 + \frac{T - t}{\tau_d}, \forall T > t \geq t_0, \tag{8}$$

where $N_\sigma(t, T)$ denotes the number of changes to (t, T).

Lemma 1 ([*45*]). *Consider a symmetric matrix $\hat{\mathcal{X}}_{33} > 0$, $\hbar(t) \in [0, h]$ and arbitrary matrices $\hat{\mathcal{X}}_{11}$, $\hat{\mathcal{X}}_{12}$, $\hat{\mathcal{X}}_{13}$, $\hat{\mathcal{X}}_{22}$, and $\hat{\mathcal{X}}_{23}$ such that $[\hat{\mathcal{X}}_{ij}]_{3 \times 3} \geq 0$, then we obtain*

$$-\int_{t-\hbar(t)}^{t} \dot{x}^T(s)\hat{\mathcal{X}}_{33}\dot{x}(s)ds \leq \int_{t-\hbar(t)}^{t} \begin{bmatrix} x(t) \\ x(t - \hbar(t)) \\ \dot{x}(s) \end{bmatrix}^T$$

$$\times \begin{bmatrix} \hat{\mathcal{X}}_{ij} & \hat{\mathcal{X}}_{12} & \hat{\mathcal{X}}_{13} \\ * & \hat{\mathcal{X}}_{22} & \hat{\mathcal{X}}_{23} \\ * & * & 0 \end{bmatrix} \begin{bmatrix} x(t) \\ x(t - \hbar(t)) \\ \dot{x}(s) \end{bmatrix} ds.$$

4. Main results

This section proposes the exponential stability criteria for the switched fuzzy system (6). The feedback control parameters of the sampled data will be derived.

Theorem 1. *For given gains $K_{j\kappa}$ and positive scalars $h_{\mathcal{U}}$, $h_{\mathcal{V}}$, α, β, and $\mu \geq 1$, the system* (6) *is stable if there exist positive symmetric matrices $P_{1\kappa} \in \mathbb{R}^{n \times n}$, $P_{1\kappa l} \in \mathbb{R}^{n \times n}$, $P_{2\kappa} \in \mathbb{R}^{n \times n}$, $P_{2\kappa l} \in \mathbb{R}^{n \times n}$, $Z_{\kappa} \in \mathbb{R}^{n \times n}$, $Z_{\kappa l} \in \mathbb{R}^{n \times n}$, and matrices $U_{11\kappa} \geq 0$, $U_{11\kappa l} \geq 0$, $U_{12\kappa} \geq 0$, $U_{12\kappa l} \geq 0$, $U_{13\kappa} \geq 0$, $U_{13\kappa l} \geq 0$, $U_{22\kappa} \geq 0$, $U_{22\kappa l} \geq 0$, $U_{23\kappa} \geq 0$, $U_{23\kappa l} \geq 0$, $U_{33\kappa} \geq 0$, $U_{33\kappa l} \geq 0$, and $\mathcal{X}_{\kappa}$, $\mathcal{X}_{\kappa l}$, $\mathcal{Y}_{\kappa}$, $\mathcal{Y}_{\kappa l}$, $\mathcal{M}_1, \mathcal{M}_2, \mathcal{M}_3, \mathcal{G}$ with appropriate dimensions satisfying the following LMIs ($\kappa \neq l \in \mathbb{S}$):*

$$\begin{cases} \Sigma_{\kappa}^A + h_{\mathcal{U}} \Sigma_{\kappa}^B < 0, \ h_k \in \{h_{\mathcal{V}}, \ h_{\mathcal{U}}\}, \\ \Sigma_{\kappa l}^A + h_{\mathcal{U}} \Sigma_{\kappa l}^B < 0, \ h_k \in \{h_{\mathcal{V}}, \ h_{\mathcal{U}}\}, \end{cases} \tag{9}$$

$$\begin{bmatrix} \Sigma_{\kappa}^A + h_k \Sigma_{\kappa}^C & \sqrt{h_k}\mathcal{M}^T \\ * & -\mathcal{Z}_{\kappa} \end{bmatrix} < 0, \ h_k \in \{h_{\mathcal{V}}, \ h_{\mathcal{U}}\}, \tag{10}$$

$$\begin{bmatrix} \Sigma_{\kappa l}^A + h_k \Sigma_{\kappa l}^C & \sqrt{h_k}\mathcal{M}^T \\ * & -\mathcal{Z}_{\kappa l} \end{bmatrix} < 0, \ h_k \in \{h_{\mathcal{V}}, \ h_{\mathcal{U}}\}, \tag{11}$$

$$\begin{cases} P_{1\kappa l} < P_{1\kappa}, \ P_{2\kappa l} < P_{1\kappa}, \ \mathcal{X}_{\kappa l} < \mathcal{X}_{\kappa}, \\ \mathcal{Y}_{\kappa l} < \mathcal{Y}_{\kappa}, \ Z_{\kappa l} < e^{-(\alpha+\beta)h_{\mathcal{U}}} Z_{\kappa}, \\ U_{11\kappa l} < U_{11\kappa}, \ U_{12\kappa l} < U_{11\kappa}, \ U_{13\kappa l} < U_{11\kappa}, \\ U_{22\kappa l} < U_{11\kappa}, \ U_{23\kappa l} < U_{11\kappa}, \ U_{33\kappa l} < U_{11\kappa}, \\ P_{1l} < \mu P_{1\kappa l}, \ P_{2l} < \mu P_{2\kappa l}, \ \mathcal{X}_l < \mu \mathcal{X}_{\kappa l}, \\ \mathcal{Y}_l < \mu \mathcal{Y}_{\kappa l}, \end{cases} \tag{12}$$

where

$$\Sigma_{\kappa}^A = e_2^T P_{1\kappa} e_1 + e_1^T P_{1\kappa}^T e_2 - [e_1 - e_3]^T P_{2\kappa} [e_1 - e_3]$$
$$+ \alpha e_1^T P_{1\kappa} e_1 - \frac{\pi^2}{4}(e_1 - e_3)^T Z_{\kappa}(e_1 - e_3)$$
$$- \begin{bmatrix} e_1 \\ e_3 \end{bmatrix}^T \begin{bmatrix} \frac{(\mathcal{X}_{\kappa} + \mathcal{X}_{\kappa}^T)}{2} & -\mathcal{X}_{\kappa} + \mathcal{Y}_{\kappa} \\ * & -\mathcal{Y}_{\kappa} - \mathcal{Y}_{\kappa}^T + \frac{(\mathcal{X}_{\kappa} + \mathcal{X}_{\kappa}^T)}{2} \end{bmatrix}$$
$$\times \begin{bmatrix} e_1 \\ e_3 \end{bmatrix} + [e_1^T \ e_2^T \ e_3^T]\mathcal{M}^T[e_1 - e_3]$$
$$+ ([e_1^T \ e_2^T \ e_3^T]\mathcal{M}^T[e_1 - e_3])^T + e_1^T [U_{13\kappa}$$
$$+ U_{13\kappa}^T]e_1 + e_1^T[-U_{13\kappa} + U_{23\kappa}]e_3$$
$$+ e_3^T[-U_{13\kappa}^T + U_{23\kappa}]e_1 + e_3^T[-U_{23\kappa} - U_{23\kappa}^T]e_3+$$
$$[e_1^T + e_2^T]\mathcal{G}[-e_2 + A_{i\kappa}e_1 + (B_{i\kappa}K_{j\kappa})e_3]$$
$$+ ([e_1^T + e_2^T]\mathcal{G}[-e_2 + A_{i\kappa}e_1 + (B_{i\kappa}K_{j\kappa})e_3])^T$$

$$\Sigma_{\kappa}^B = [e_1 - e_3]^T P_{2\kappa} e_2 + e_2^T P_{2\kappa}^T [e_1 - e_3]$$
$$+ \alpha[e_1 - e_3]^T P_{2\kappa}[e_1 - e_3] + e_2^T Z_{\kappa} e_2 + \alpha \begin{bmatrix} e_1 \\ e_3 \end{bmatrix}^T$$
$$\times \begin{bmatrix} \frac{(\mathcal{X}_{\kappa} + \mathcal{X}_{\kappa}^T)}{2} & -\mathcal{X}_{\kappa} + \mathcal{Y}_{\kappa} \\ * & -\mathcal{Y}_{\kappa} - \mathcal{Y}_{\kappa}^T + \frac{(\mathcal{X}_{\kappa} + \mathcal{X}_{\kappa}^T)}{2} \end{bmatrix} \begin{bmatrix} e_1 \\ e_3 \end{bmatrix}$$
$$+ \left[e_2^T \frac{\mathcal{X}_{\kappa} + \mathcal{X}_{\kappa}^T}{2} e_1 + e_1^T \left(\frac{\mathcal{X}_{\kappa} + \mathcal{X}_{\kappa}^T}{2} \right)^T e_2 \right]$$
$$+ \left[e_2^T(-\mathcal{X}_{\kappa} + \mathcal{Y}_{\kappa})e_3 + e_3^T \left(-\mathcal{X}_{\kappa} + \mathcal{Y}_{\kappa} \right)^T e_2 \right],$$

$$\Sigma_{\kappa}^C = e_1^T U_{11\kappa} e_1 + e_1^T U_{12\kappa} e_3 + e_3^T U_{12\kappa}^T e_1 - e_3^T U_{12\kappa}^T e_3,$$

$$\Sigma_{\kappa l}^A = e_2^T P_{1\kappa l} e_1^T + e_1^T P_{1\kappa l}^T e_2 - [e_1 - e_3]^T P_{2\kappa l}[e_1 - e_3]$$
$$+ \alpha e_1^T P_{1\kappa l} e_1 - \frac{\pi^2}{4}(e_1 - e_3)^T Z_{\kappa l}(e_1 - e_3)$$
$$- \begin{bmatrix} e_1 \\ e_3 \end{bmatrix}^T \begin{bmatrix} \frac{(\mathcal{X}_{\kappa l} + \mathcal{X}_{\kappa l}^T)}{2} & -\mathcal{X}_{\kappa l} + \mathcal{Y}_{\kappa l} \\ * & -\mathcal{Y}_{\kappa l} - \mathcal{Y}_{\kappa l}^T + \frac{(\mathcal{X}_{\kappa l} + \mathcal{X}_{\kappa l}^T)}{2} \end{bmatrix}$$
$$\times \begin{bmatrix} e_1 \\ e_3 \end{bmatrix} + [e_1^T \ e_2^T \ e_3^T]\mathcal{M}^T$$
$$\times [e_1 - e_3] + ([e_1^T \ e_2^T \ e_3^T]\mathcal{M}^T[e_1 - e_3])^T$$
$$+ e_1^T[U_{13\kappa l} + U_{13\kappa l}^T]e_1 + e_1^T[-U_{13\kappa l} + U_{23\kappa l}^T]e_3$$
$$+ e_3^T[-U_{13\kappa l}^T + U_{23\kappa l}]e_1 + e_3^T[-U_{23\kappa l} - U_{23\kappa l}^T]e_3$$

$$+ [e_1^T + e_2^T]\mathcal{G}[-e_2 + A_{i\kappa l}e_1 + (B_{i\kappa l}K_{j\kappa l})e_3]$$
$$+ ([e_1^T + e_2^T]\mathcal{G}[-e_2 + A_{i\kappa l}e_1 + (B_{i\kappa l}K_{j\kappa l})e_3])^T,$$

$$\Sigma_{\kappa l}^B = [e_1 - e_3]^T P_{2\kappa l} e_2 + e_2^T P_{2\kappa l}^T [e_1 - e_3]$$
$$+ \alpha[e_1 - e_3]^T P_{2\kappa l}[e_1 - e_3] + e_2^T Z_{\kappa l} e_2$$
$$+ \alpha \begin{bmatrix} e_1 \\ e_3 \end{bmatrix}^T \begin{bmatrix} \frac{(\mathcal{X}_{\kappa l} + \mathcal{X}_{\kappa l}^T)}{2} & -\mathcal{X}_{\kappa l} + \mathcal{Y}_{\kappa l} \\ * & -\mathcal{Y}_{\kappa l} - \mathcal{Y}_{\kappa l}^T + \frac{(\mathcal{X}_{\kappa l} + \mathcal{X}_{\kappa l}^T)}{2} \end{bmatrix}$$
$$\times \begin{bmatrix} e_1 \\ e_3 \end{bmatrix} + \left[e_2^T \frac{\mathcal{X}_{\kappa l} + \mathcal{X}_{\kappa l}^T}{2} e_1 + e_1^T \left(\frac{\mathcal{X}_{\kappa l} + \mathcal{X}_{\kappa l}^T}{2} \right)^T e_2 \right]$$
$$+ \left[e_2^T(-\mathcal{X}_{\kappa l} + \mathcal{Y}_{\kappa l})e_3 + e_3^T \left(-\mathcal{X}_{\kappa l} + \mathcal{Y}_{\kappa l} \right)^T e_2 \right],$$

$$\Sigma_{\kappa l}^C = e_1^T U_{11\kappa l} e_1 + e_1^T U_{12\kappa l} e_3 + e_3^T U_{12\kappa l}^T e_1 - e_3^T U_{12\kappa l}^T e_3,$$

and $e_j = [0_{n \times (j-1)n}, \ I_n \ 0_{n \times (3-j)n}], j = 1, 2, 3,$

and if the average dwell time (ADT), τ_a of the switching signal satisfies

$$\tau_a > \frac{(\alpha + \beta)h_{\mathcal{U}} + \ln\mu}{\alpha}. \tag{13}$$

Proof. (See Appendix for a proof). □

5. Sampled-data stabilization

In this section, the adequate condition acquired in Theorem 1 cannot be formulated with respect to LMIs due to the presence of non-linear terms. In such a manner, we will provide a co-design method for the controller gains of the fuzzy SDC, which can determine the following theorem.

Theorem 2. *For any given positive scalars $h_{\mathcal{U}}$, $h_{\mathcal{V}}$, α, β, and $\mu \geq 1$, the system* (6) *is asymptotically stable, if there exist positive definite matrices $\overline{P}_{1\kappa} \in \mathbb{R}^{n \times n}$, $\overline{P}_{1\kappa l} \in \mathbb{R}^{n \times n}$, $\overline{P}_{2\kappa} \in \mathbb{R}^{n \times n}$, $\overline{P}_{2\kappa l} \in \mathbb{R}^{n \times n}$, $\overline{Z}_{\kappa} \in \mathbb{R}^{n \times n}$, $\overline{Z}_{\kappa l} \in \mathbb{R}^{n \times n}$, and matrices $\overline{Z}_{11\kappa} \geq 0$, $\overline{Z}_{11\kappa l} \geq 0$, $\overline{Z}_{12\kappa} \geq 0$, $\overline{Z}_{12\kappa l} \geq 0$, $\overline{Z}_{13\kappa} \geq 0$, $\overline{Z}_{13\kappa l} \geq 0$, $\overline{Z}_{22\kappa} \geq 0$, $\overline{Z}_{22\kappa l} \geq 0$, $\overline{Z}_{23\kappa} \geq 0$, $\overline{Z}_{23\kappa l} \geq 0$, $\overline{Z}_{33\kappa} \geq 0$, $\overline{Z}_{33\kappa l} \geq 0$, and $\overline{\mathcal{X}}_{\kappa}$, $\overline{\mathcal{X}}_{\kappa l}$, $\overline{\mathcal{Y}}_{\kappa}$, $\overline{\mathcal{Y}}_{\kappa l}$, $\overline{\mathcal{M}}_1, \overline{\mathcal{M}}_2, \overline{\mathcal{M}}_3, \overline{\mathcal{G}}$ with appropriate dimensions satisfying the following LMIs ($\kappa \neq l \in \mathbb{S}$);*

$$\begin{cases} \overline{\Sigma}_{\kappa}^A + h_{\mathcal{U}} \overline{\Sigma}_{\kappa}^B < 0, \ h_k \in \{h_{\mathcal{V}}, \ h_{\mathcal{U}}\}, \\ \overline{\Sigma}_{\kappa l}^A + h_{\mathcal{U}} \overline{\Sigma}_{\kappa l}^B < 0, \ h_k \in \{h_{\mathcal{V}}, \ h_{\mathcal{U}}\}, \end{cases} \tag{14}$$

$$\begin{bmatrix} \overline{\Sigma}_{\kappa}^A + h_k \overline{\Sigma}_{\kappa}^C & \sqrt{h_k}\overline{\mathcal{M}}^T \\ * & -\overline{\mathcal{Z}}_{\kappa} \end{bmatrix} < 0, \tag{15}$$

$$\begin{bmatrix} \overline{\Sigma}_{\kappa l}^A + h_k \overline{\Sigma}_{\kappa l}^C & \sqrt{h_k}\overline{\mathcal{M}}^T \\ * & -\overline{\mathcal{Z}}_{\kappa l} \end{bmatrix} < 0, \tag{16}$$

$$\begin{cases} \overline{P}_{1\kappa l} < \overline{P}_{1\kappa}, \ \overline{P}_{2\kappa l} < \overline{P}_{1\kappa}, \ \overline{\mathcal{X}}_{\kappa l} < \overline{\mathcal{X}}_{\kappa}, \\ \overline{\mathcal{Y}}_{\kappa l} < \overline{\mathcal{Y}}_{\kappa}, \ \overline{Z}_{\kappa l} < e^{-(\alpha+\beta)h_{\mathcal{U}}} \overline{Z}_{\kappa}, \\ \overline{Z}_{11\kappa l} < \overline{Z}_{11\kappa}, \ \overline{Z}_{12\kappa l} < \overline{Z}_{11\kappa}, \\ \overline{Z}_{13\kappa l} < \overline{Z}_{11\kappa}, \ \overline{Z}_{22\kappa l} < \overline{Z}_{11\kappa}, \\ \overline{Z}_{23\kappa l} < \overline{Z}_{11\kappa}, \ \overline{Z}_{33\kappa l} < \overline{Z}_{11\kappa}, \\ \overline{P}_{1l} < \mu \overline{P}_{1\kappa l}, \ \overline{P}_{2l} < \mu \overline{P}_{2\kappa l}, \\ \overline{\mathcal{X}}_l < \mu \overline{\mathcal{X}}_{\kappa l}, \ \overline{\mathcal{Y}}_l < \mu \overline{\mathcal{Y}}_{\kappa l}, \end{cases} \tag{17}$$

where

$$\overline{\Sigma}_{\kappa}^A = e_2^T \overline{P}_{1\kappa} e_1 + e_1^T \overline{P}_{1\kappa}^T e_2 - [e_1 - e_3]^T \overline{P}_{2\kappa}[e_1 - e_3]$$
$$+ \alpha e_1^T \overline{P}_{1\kappa} e_1 - \frac{\pi^2}{4}(e_1 - e_3)^T \overline{Z}_{\kappa}(e_1 - e_3)$$
$$- \begin{bmatrix} e_1 \\ e_3 \end{bmatrix}^T \overline{\prod} \begin{bmatrix} e_1 \\ e_3 \end{bmatrix} + [e_1^T \ e_2^T \ e_3^T]\overline{\mathcal{M}}^T[e_1 - e_3]$$
$$+ ([e_1^T \ e_2^T \ e_3^T]\overline{\mathcal{M}}^T[e_1 - e_3])^T + e_1^T[\overline{Z}_{13\kappa} + \overline{Z}_{13\kappa}^T]e_1$$
$$+ e_1^T[-\overline{Z}_{13\kappa} + \overline{Z}_{23\kappa}^T]e_3 + e_3^T[-\overline{Z}_{13\kappa}^T + \overline{Z}_{23\kappa}]e_1$$

$$+ e_3^T[-\overline{Z}_{23\kappa} - \overline{Z}_{23\kappa}^T]e_3 + [e_1^T + e_2^T]$$
$$\times [-\overline{\mathcal{G}}e_2 + A_{i\kappa}\overline{\mathcal{G}}e_1 + (B_{i\kappa}H_{j\kappa})e_3]$$
$$+ ([e_1^T + e_2^T][-\overline{\mathcal{G}}e_2 + A_{i\kappa}\overline{\mathcal{G}}e_1 + (B_{i\kappa}H_{j\kappa})e_3])^T$$

$$\overline{\Sigma}_\kappa^B = [e_1 - e_3]^T\overline{P}_{2\kappa}e_2 + e_2^T\overline{P}_{2\kappa}^T[e_1 - e_3]$$
$$+ \alpha[e_1 - e_3]^T\overline{P}_{2\kappa}[e_1 - e_3] + e_2^T\overline{Z}_\kappa e_2$$
$$+ \alpha \begin{bmatrix} e_1 \\ e_3 \end{bmatrix}^T \overline{\amalg} \begin{bmatrix} e_1 \\ e_3 \end{bmatrix}$$
$$+ \left[e_2^T \frac{\overline{\mathcal{X}}_\kappa + \overline{\mathcal{X}}_\kappa^T}{2} e_1 + e_1^T \left(\frac{\overline{\mathcal{X}}_\kappa + \overline{\mathcal{X}}_\kappa^T}{2} \right)^T e_2 \right]$$
$$+ \left[e_2^T(-\overline{\mathcal{X}}_\kappa + \overline{\mathcal{Y}}_\kappa)e_3 + e_3^T \left(-\overline{\mathcal{X}}_\kappa + \overline{\mathcal{Y}}_\kappa \right)^T e_2 \right],$$

$$\overline{\Sigma}_\kappa^C = e_1^T\overline{Z}_{11\kappa}e_1 + e_1^T\overline{Z}_{12\kappa}e_3 + e_3^T\overline{Z}_{12\kappa}^Te_1 - e_3^T\overline{Z}_{12\kappa}^Te_3,$$

$$\overline{\Sigma}_{\kappa l}^A = e_2^T\overline{P}_{1\kappa l}e_1^T + e_1^T\overline{P}_{1\kappa l}^Te_2 - [e_1 - e_3]^T\overline{P}_{2\kappa l}[e_1 - e_3]$$
$$+ \alpha e_1^T\overline{P}_{1\kappa l}e_1 - \frac{\pi^2}{4}(e_1 - e_3)^T\overline{Z}_{\kappa l}(e_1 - e_3)$$
$$- \begin{bmatrix} e_1 \\ e_3 \end{bmatrix}^T \overline{\amalg} \begin{bmatrix} e_1 \\ e_3 \end{bmatrix} + [e_1^T \ e_2^T \ e_3^T]\overline{\mathcal{M}}^T[e_1 - e_3]$$
$$+ ([e_1^T \ e_2^T \ e_3^T]\overline{\mathcal{M}}^T[e_1 - e_3])^T$$
$$+ e_1^T[\overline{Z}_{13\kappa l} + \overline{Z}_{13\kappa l}^T]e_1$$
$$+ e_1^T[-\overline{Z}_{13\kappa l} + \overline{Z}_{23\kappa l}^T]e_3 + e_3^T[-\overline{Z}_{13\kappa l}^T + \overline{Z}_{23\kappa l}]e_1$$
$$+ e_3^T[-\overline{Z}_{23\kappa l} - \overline{Z}_{23\kappa l}^T]e_3$$
$$+ [e_1^T + e_2^T][-\overline{\mathcal{G}}e_2 + A_{i\kappa l}\overline{\mathcal{G}}e_1 + (B_{i\kappa l}H_{j\kappa l})e_3]$$
$$+ ([e_1^T + e_2^T][-\overline{\mathcal{G}}e_2 + A_{i\kappa l}\overline{\mathcal{G}}e_1 + (B_{i\kappa l}H_{j\kappa l})e_3])^T$$

$$\overline{\Sigma}_{\kappa l}^B = [e_1 - e_3]^T\overline{P}_{2\kappa l}e_2 + e_2^T\overline{P}_{2\kappa l}^T[e_1 - e_3]$$
$$+ \alpha[e_1 - e_3]^T\overline{P}_{2\kappa l}[e_1 - e_3] + e_2^T\overline{Z}_{\kappa l}e_2$$
$$+ \alpha \begin{bmatrix} e_1 \\ e_3 \end{bmatrix}^T \overline{\amalg} \begin{bmatrix} e_1 \\ e_3 \end{bmatrix}$$
$$+ \left[e_2^T \frac{\overline{\mathcal{X}}_{\kappa l} + \overline{\mathcal{X}}_{\kappa l}^T}{2} e_1 + e_1^T \left(\frac{\overline{\mathcal{X}}_{\kappa l} + \overline{\mathcal{X}}_{\kappa l}^T}{2} \right)^T e_2 \right]$$
$$+ \left[e_2^T(-\overline{\mathcal{X}}_{\kappa l} + \overline{\mathcal{Y}}_{\kappa l})e_3 + e_3^T \left(-\overline{\mathcal{X}}_{\kappa l} + \overline{\mathcal{Y}}_{\kappa l} \right)^T e_2 \right],$$

$$\overline{\Sigma}_{\kappa l}^C = e_1^T\overline{Z}_{11\kappa l}e_1 + e_1^T\overline{Z}_{12\kappa l}e_3 + e_3^T\overline{Z}_{12\kappa l}^Te_1 - e_3^T\overline{Z}_{12\kappa l}^Te_3,$$

$$\text{and } e_J = [0_{n\times(J-1)n}, \quad I_n \quad 0_{n\times(3-J)n}], J = 1, 2, 3,$$

$$\overline{\amalg} = \begin{bmatrix} \frac{(\overline{\mathcal{X}}_\kappa + \overline{\mathcal{X}}_\kappa^T)}{2} & -\overline{\mathcal{X}}_\kappa + \overline{\mathcal{Y}}_\kappa \\ * & -\overline{\mathcal{Y}}_\kappa - \overline{\mathcal{Y}}_\kappa^T + \frac{(\overline{\mathcal{X}}_\kappa + \overline{\mathcal{X}}_\kappa^T)}{2} \end{bmatrix} \text{ and if the average dwell-time,}$$

τ_a of switching signal satisfies

$$\tau_a > \frac{(\alpha + \beta)h_{\mathcal{U}} + In\mu}{\alpha}. \tag{18}$$

Moreover, the gains of the controller are given by $K_{j\kappa} = \overline{\mathcal{H}}_{j\kappa}\overline{\mathcal{G}}^{-1}$.

Proof. Let $\overline{\mathcal{G}} = \mathcal{G}^{-1}$, $\Lambda = \text{diag}\{\overline{\mathcal{G}}, \overline{\mathcal{G}}, \overline{\mathcal{G}}\}$,
$\Lambda_1 = \text{diag}\{\overline{\mathcal{G}}, \overline{\mathcal{G}}, \overline{\mathcal{G}}, \overline{\mathcal{G}}\}$, $\overline{P}_{1\kappa} = \overline{\mathcal{G}}P_{1\kappa}\overline{\mathcal{G}}$, $\overline{P}_{2\kappa} = \overline{\mathcal{G}}P_{2\kappa}\overline{\mathcal{G}}$, $\overline{Z}_\kappa = \overline{\mathcal{G}}Z_\kappa\overline{\mathcal{G}}$, $\overline{U}_{11\kappa} = \overline{\mathcal{G}}U_{11\kappa}\overline{\mathcal{G}}$, $\overline{U}_{12\kappa} = \overline{\mathcal{G}}U_{12\kappa}\overline{\mathcal{G}}$, $\overline{U}_{13\kappa} = \overline{\mathcal{G}}U_{13\kappa}\overline{\mathcal{G}}$,
$\overline{U}_{22\kappa} = \overline{\mathcal{G}}U_{22\kappa}\overline{\mathcal{G}}$, $\overline{U}_{23\kappa} = \overline{\mathcal{G}}U_{23\kappa}\overline{\mathcal{G}}$, $\overline{U}_{33\kappa} = \overline{\mathcal{G}}U_{33\kappa}\overline{\mathcal{G}}$, $\overline{\mathcal{X}}_\kappa = \overline{\mathcal{G}}\mathcal{X}_\kappa\overline{\mathcal{G}}$, $\overline{\mathcal{Y}}_\kappa = \overline{\mathcal{G}}\mathcal{Y}_\kappa\overline{\mathcal{G}}$, $\overline{\mathcal{M}}_{1\kappa} = \overline{\mathcal{G}}\mathcal{M}_{1\kappa}\overline{\mathcal{G}}$, $\overline{\mathcal{M}}_{2\kappa} = \overline{\mathcal{G}}\mathcal{M}_{2\kappa}\overline{\mathcal{G}}$,
$\overline{\mathcal{M}}_{3\kappa} = \overline{\mathcal{G}}\mathcal{M}_{3\kappa}\overline{\mathcal{G}}$. Left and right multiplying (9) by Λ and (10)–(11) by Λ_1, it can be shown that the inequalities (14)–(16) hold. $\square$

Remark 1. Theorems 1 and 2 ensure stability and stabilization conditions according to the time-dependent switched LKF for the system (8) with respect to the switched SDC. With the aim of demonstrating the performance of novel LKF, we consider the following LKF without

switching conditions as follows:

$$V(t) = \sum_{d=1}^{3} V_d(t), \ t \in [t_k, t_{k+1}), \tag{19}$$

where

$$V_{\kappa 1}(t) = x^T(t)P_1x(t)$$
$$+ (t_{k+1} - t)[x(t) - x(t_k)]^T P_2[x(t) - x(t_k)],$$

$$V_{\kappa 2}(t) = (t_{k+1} - t) \begin{bmatrix} x(t) \\ x(t_k) \end{bmatrix}^T \overbrace{\amalg} \begin{bmatrix} x(t) \\ x(t_k) \end{bmatrix},$$

$$V_{\kappa 3}(t) = (t_{k+1} - t) \int_{t_k}^t e^{\alpha(s-t)}\dot{x}^T(s)Z\dot{x}(s)ds$$
$$- \frac{\pi^2}{4} \int_{t_k}^t e^{\alpha(s-t)}(x(s) - x(t_k))^T Z(x(s) - x(t_k))ds.$$

Theorems 1–2 contain the sufficient condition for system (8) by taking into account the identical LKF and the controller gains are $K_j = \overline{\mathcal{H}}_j\overline{\mathcal{G}}^{-1}$.

Remark 2. The derived conditions of Theorem 1 can be utilized to investigate the system (6) under a given control gain, and the requirements of Theorem 2 can be utilized to plan a control gain that stabilizes the system (6). Furthermore, to infer the LMI-based stabilization conditions of Theorem 1 from Theorem 2, $\overline{\mathcal{G}}$ assumes a vital role in the change of the LMIs through the congruent transformation approach. In addition, we plan a TSFSD controller by utilizing parallel distributed compensation (PDC) technology and LMIs. The TSFSD controller model can guarantee exponential stability of the switched system.

Remark 3. According to Theorem 2, no matter what the switching rule is, the intended controller remains the same. That is, the modeled controller does not need to be altered every time the chaotic systems switch. As the switching law $\sigma(t)$ is arbitrary, for the switched chaotic system (6) with the Lorenz system ($\delta = [0, 0.8)$), Chen system ($\delta = (0.8, 1]$), and the Lu system ($\delta = 0.8$), the following stitching law is defined to choose the chaotic system every time.

$$\sigma(t) = \begin{cases} 1, \ell \in [\ell_{3n}, \ell_{3n+1}), \ell_{3n+1} - \ell_{3n} = rand, \\ 3, \ell \in [\ell_{3n+1}, \ell_{3n+2}), \ell_{3n+2} - \ell_{3n+1} = rand, \\ 2, \ell \in [\ell_{3n+2}, \ell_{3n+3}), \ell_{3n+3} - \ell_{3n+2} = rand, \end{cases} \tag{20}$$

where $m \geq 0$; 1, 2, and 3 denotes the Lorenz system, Lu system, Chen system, respectively. *rand* denotes the active time of every subsystem that being arbitrary.

Remark 4. It is important to note that very limited works have been done on exponentially stable for T–S fuzzy chaotic system with sampled-data controller (SDC) based on the information of switching signal with input delay. It is noteworthy that in many industrial processes, the dynamical behaviors are generally complex and non-linear and their genuine mathematical models are always difficult to obtain. In [46], a procedure is proposed for the design of a sampled-data controller is proposed for T–S fuzzy chaotic system. Authors in [47], formulated periodic sampled-data stabilization of chaotic systems with the fuzzy approach. Stabilization analysis for fuzzy systems with a switched sampled-data control has been discussed in [39]. The model considered in this present study is more practical than that proposed by [39,46,47], in light of the fact that they consider the usual SDC to have been studied with T–S fuzzy nonlinear system, but in this paper, we consider a fuzzy SDC with information about the switching signal. However, the authors in [39,46,47] used some simple techniques to LKFs to solve the stability problems to those articles. In this paper, a novel LKF with information about the switching signal and the input delay approach has been proposed for the exponential stability analysis of the T–S fuzzy system. In addition, we have analyzed all
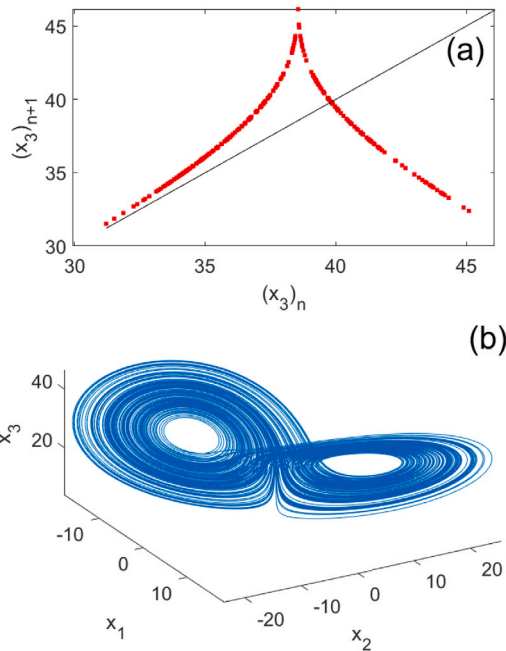
Fig. 1. (a) Poincar'e section in the Lorenz attractor at $\delta = 0.01$, $\rho = 28$ in the $(x_3)_n$ vs. $(x_3)_{n+1}$ plane, and the corresponding (b) three-dimensional chaotic attractor.

the families of systems (Lorentz system: $\delta \in [0, 0.8)$, Chen family: $\delta \in (0.8, 1]$, Lu system: $\delta = 0.8$) in the numerical example section. However, those methods cannot be applied to these systems with SDC. Therefore the analysis technique and system model proposed in this paper is more general than [39,46,47], which differentiates our work more effectively and this was demonstrate by the numerical simulation examples. Hence, the results presented in this paper is essentially new.

6. Examples

In this section, illustrative examples have been provided to illustrate the validity of the established theoretical approaches using SDC.

Example 6.1. Consider the following a chaotic system as transmitter:

$$\begin{cases} \dot{x}_1(t) = (25\delta + 10)(x_2(t) - x_1(t)) + u(t), \\ \dot{x}_2(t) = (\rho - 35\delta)x_1(t) + (29\delta - 1)x_2(t) - x_1(t)x_3(t), \\ \dot{x}_3(t) = x_1(t)x_2(t) - \left(\frac{8+\delta}{3}\right)x_3(t), \end{cases} \quad (21)$$

where δ is an abrupt single-key parameter, we fix ρ as the system controlling independent parameter to identify the period doubling phenomenon. In this manuscript, we fix the parameter $\rho = 28$ for the above system (21). Consider the unified chaotic system (21), when $\delta \in [0, 0.8)$, it is called the Lorentz system; when $\delta \in (0.8, 1]$ it is called the Chen system; when $\delta = 0.8$, it is called the Lu system. In this part, the switched chaotic system (2) is comprised by these three chaotic systems, i.e., $m = 3$. $\kappa = 1$ denotes the Lorenz system; $\kappa = 2$ denotes the Lu system; $\kappa = 3$ denotes the Chen system.

6.1. Lorentz system: $\delta \in [0, 0.8)$

To investigate the Lorenz system under $\delta \in [0, 0.8)$ parameter range, the maxima of x_3 is obtained to find the symmetry and the changes in the wings of the chaotic attractor. The Poincaré return map is plotted between $(x_3)_n$ vs $(x_3)_{n+1}$ with the above-mentioned parameters. The resulting graph is shown in Fig. 1(a). The corresponding double-wing chaotic attractor in a three-dimensional plane is shown in Fig. 1(b). Notice that from the Poincar'e analysis, the slope values (magnitude)
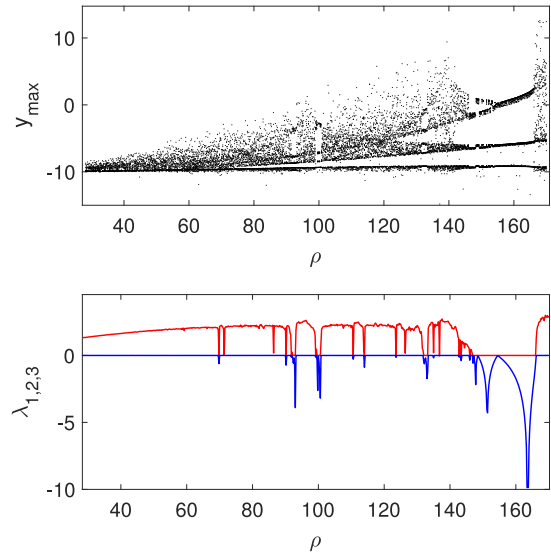

Fig. 2. Numerically computed (upper panel) bifurcation diagram and its corresponding (lower panel) Lyapunov exponent spectrum with respect to the parameter $\rho \in (140, 150)$. Note that the plot computed by fixing the transformation parameter $\delta = 0.01$.
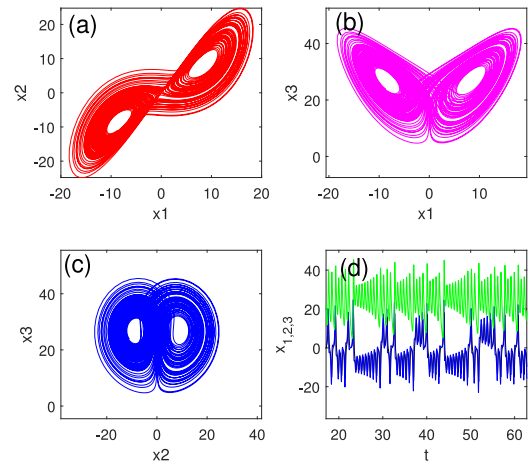

Fig. 3. Numerically computed double-wing chaotic Lorenz system in different projections. (a) $x_1 - x_2$, (b) $x_1 - x_3$, (c) $x_2 - x_3$ planes and corresponding time series of the variables (d) x_1, x_2, and x_3.

of the graph are greater than one throughout the range visited by the double-wing trajectory. This is an indication that the system has a positive Lyapunov exponent and proves that the system exhibits chaos. The calculation of the Lyapunov exponent and its corresponding bifurcations is shown in Fig. 2. The period was doubling in the range of $\rho \in (140, 150)$. Changes in the sign of the Lyapunov exponent (λ_1 red color) also promise the same. For the sake of simplicity, the third large magnitude of negative Lyapunov exponent (λ_3) is avoided here. The symmetry about zero in the Poincar'e map shows that the two wings of the chaotic attractor are mirror-like structures (two wings). Notice that the Poincaré obtained considered the section $\dot{x}_3 = 0$. For more clarity, the different projections of the chaotic attractor are plotted in Fig. 3. From this different projection, the symmetrical wing is visualized. The frequency of chaotic data calculated using the discrete Fourier transform (DFT) of the x_1 signal using a fast Fourier transform (FFT) algorithm is shown in Fig. 4. It is shown that the broad-band spectrum (multiple frequencies) of frequency domains is shown to represents the chaotic nature of the signal. Note that the transformation parameter δ is set to 0.01 in this case.
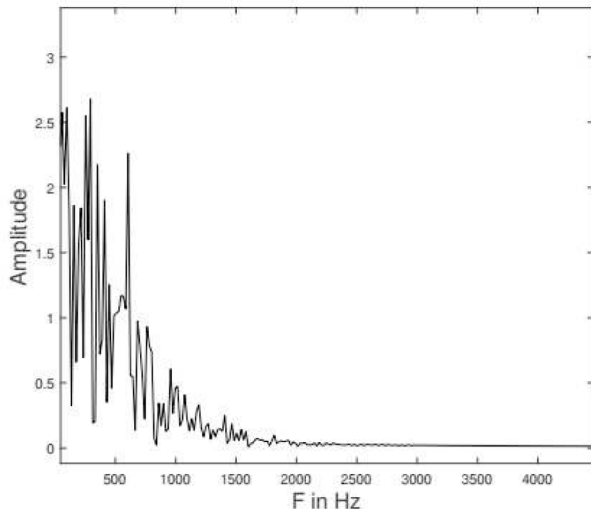
Fig. 4. The FFT measurement of the signal x_1 is based on the Discrete Fourier Transform (DFT). x-axis the frequency and the y-axis is the amplitude of the signal.

Fig. 6. Numerically computed double wing chaotic Chen system in the different projections. (a) $x_1 - x_2$, (b) $x_1 - x_3$, (c) $x_2 - x_3$ planes and corresponding time series of the variables (d) x_1, x_2, x_3.

Fig. 5. Numerically computed (upper panel) bifurcation diagram and its corresponding (lower panel) Lyapunov exponent spectrum with respect to the parameter ρ. Note that the plot computed by fixing the transformation parameter $\delta = 0.85$.

Fig. 7. The FFT measurement of the signal x_1 is based on the Discrete Fourier Transform (DFT). x-axis the frequency and the y-axis is the amplitude of the signal.
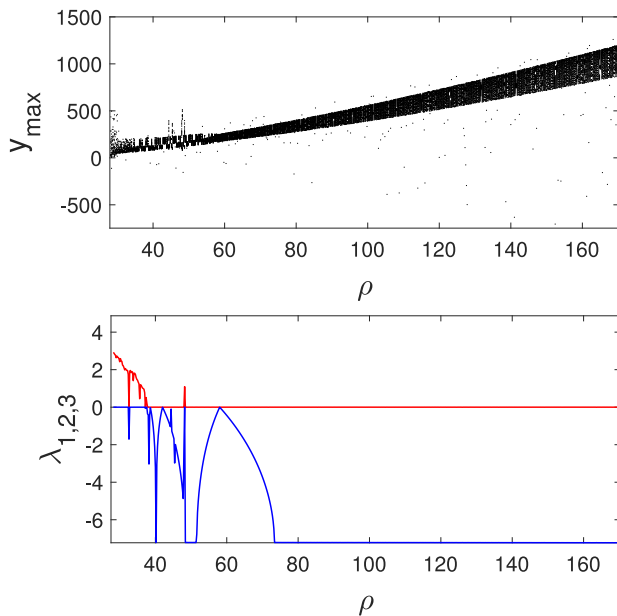
6.2. Chen family: $\delta \in (0.8, 1]$

Here, the symmetrical nature of the double band chaotic attractor is investigated by fixing the transformation parameter $\delta = 0.85$. The calculation of the Poincaré return map is the same here.

Fig. 12 shows the Poincaré return map, which is plotted between $(x_3)_n$ vs $(x_3)_{n+1}$ with the above-mentioned parameters by fixing $\delta = 0.85$. The resulting graph is shown in Fig. 12(a). The corresponding double wing chaotic attractor in a three dimensional plane which is shown in Fig. 12(b). Notice that from the Poincaré analysis, the slope values (magnitude) of the graph is not smooth and we get another line from the hump. which means the range visited by the double wing trajectory is not symmetrical and creates a new wing inside the two wings of the trajectories. The symmetry is not zero on this Poincar'e map. This is an indication of the Chen family of attractors. The change
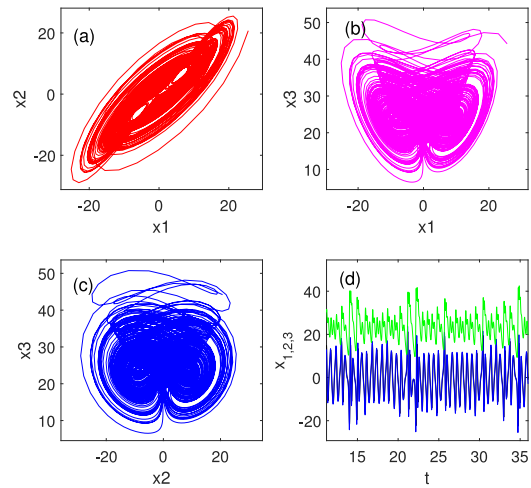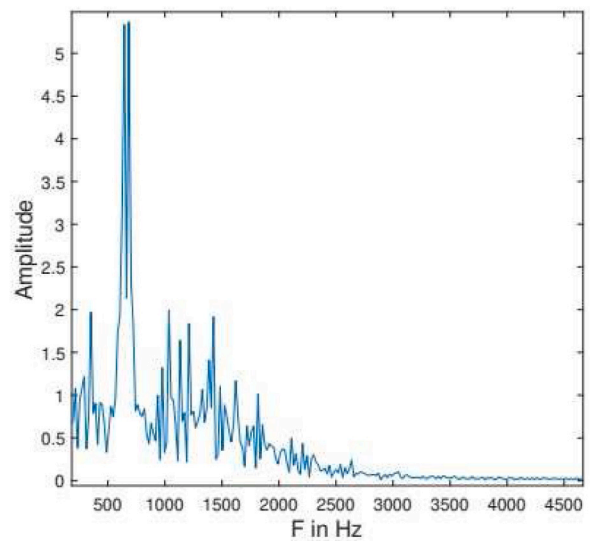
in dynamics is due to the transformation parameter α. Fig. 5 shows the Lyapunov exponent and its corresponding bifurcation plots. The period is achieved as a double in the range of $\rho \in (40, 60)$. Changes in the sign of the Lyapunov exponent (λ_1 red color) also promise the same. For the sake of simplicity, the third large magnitude of the negative Lyapunov exponent (λ_3) is avoided here. Notice that the Poincaré obtained considered the section $\dot{x}_3 = 0$, similar to the Lorenz case. For more clarity, the different projections of the chaotic attractor are plotted in Fig. 6. From this different projection, the nonsymmetrical wing is visualized. The frequency of chaotic data calculated using the discrete Fourier transform (DFT) of the x_1 signal using a fast Fourier transform algorithm (FFT) is shown in Fig. 7. The broad-band spectrum (multiple frequencies) of frequency domains represents the chaotic nature of the signal. The frequency components are greater than the frequency domain of the Lorenz System, representing the transformation of the dynamics. Note that the transformation parameter δ is set to 0.85 in this case.
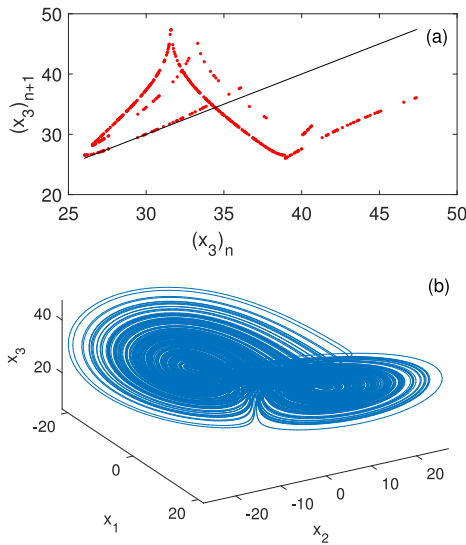
Fig. 8. (a) Poincar'e section in the Lu attractor at $\delta = 0.8$, $\rho = 28$ in the $(x_3)_n$ vs. $(x_3)_{n+1}$ plane and corresponding (b) three-dimensional chaotic attractor.
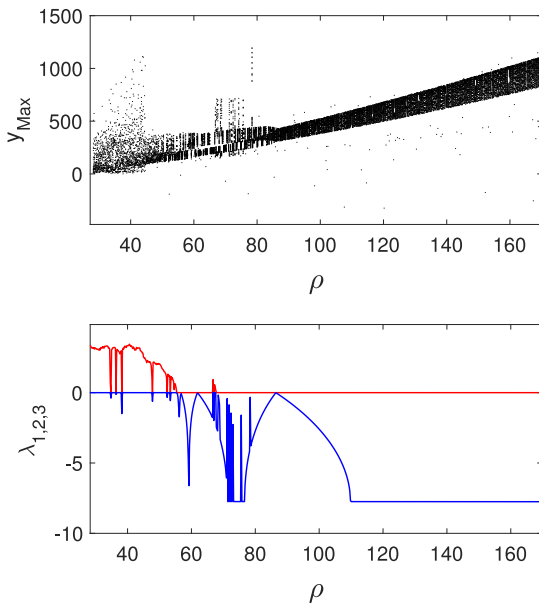

Fig. 9. Numerically computed (upper panel) bifurcation diagram and its corresponding (lower panel) Lyapunov exponent spectrum with respect to the parameter ρ. Note that the plot computed by fixing the transformation parameter $\delta = 0.8$.

6.3. Lu system: $\delta = 0.8$

Here, the symmetrical nature of the double band chaotic attractor is investigated by fixing the transformation parameter $\delta = 0.8$. The calculation of the Poincar'e return map is the same here as in the earlier notes. Fig. 8 shows the Poincar'e return map, which is plotted between $(x_3)_n$ vs. $(x_3)_{n+1}$ with the parameters mentioned above by fixing $\delta = 0.8$. The resulting graph is shown in Fig. 8(a). The corresponding double wing chaotic attractor in a three dimensional plane which is shown in Fig. 8(b). Notice that from the Poincaré analysis the slope values (magnitude) of the graph is not smooth and random from the original hump. which means the range visited by the double wing trajectory is not symmetrical and creates a new wing inside the two wings of

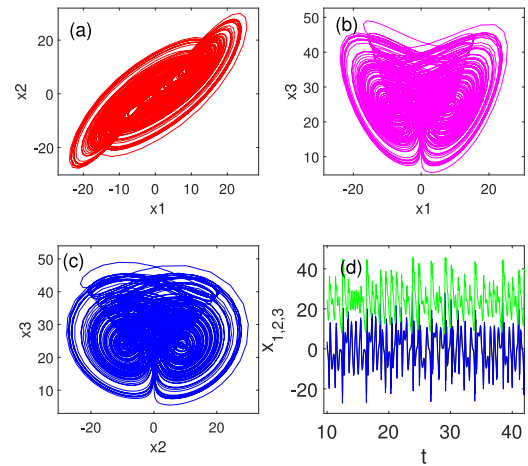

Fig. 10. Numerically computed double wing chaotic Chen system in the different projections. (a) $x_1 - x_2$, (b) $x_1 - x_3$, (c) $x_2 - x_3$ planes and corresponding time series of the variables (d) x_1, x_2, x_3.

the trajectories 8(b). The symmetry is not zero on this Poincar'e map. This is an indication of the Lu family of attractors. The change in dynamics is due to the transformation parameter δ. Fig. 9 shows the Lyapunov exponent and its corresponding bifurcation plots. Double period achieved in the range of $\rho \in (60, 80)$. Changes in the sign of the Lyapunov exponent (λ_1 red color) also promisealso promisecolorcolor) also promise the same. For the sake of simplicity, the third large magnitude of negative Lyapunov exponent (λ_3) is avoided here. Notice that the Poincaré obtained considered the section $\dot{x}_3 = 0$ similar to the Lorenz and Chen system. For more clarity, the different projections of the chaotic Lu attractor are plotted in Fig. 10. From this different projection, the nonsymmetrical wing is visualized. The frequency of chaotic data calculated using the discrete Fourier transform (DFT) of the x_1 signal using a fast Fourier transform algorithm (FFT) is shown in Fig. 11. The broad band spectrum (multiple frequency) of frequency domains is shown to represent the chaotic nature of the signal. The frequency components are greater than the frequency domains of the Lorenz and Chen Systems. which represents the transformation of the dynamics. Notice that in the frequency spectra, there is one notable harmonic that falls into the newly born wing in between the chaotic attractor. Furthermore, the transformation parameter δ is set to 0.8 in this case.

The system (21) is the well-known Lorenz, Lu, and Chen chaotic systems, when $\delta = \{0, 0.8, 1\}$, respectively. The state variable $x(0) \in [-10, 10, 10]^T$, utilizing T–S fuzzy modeling approach:

$$\dot{x}(t) = \sum_{i=1}^{2} h_i(x(t))\left[A_{i\kappa}x(t) + B_{i\kappa}u(t)\right], \tag{22}$$

where $x = [x_1, x_2, x_3]^T$. Now, putting the circuit equation into the state–space format, we have the following systems, which are continuously connected together:

When $\delta = 0$, the above chaotic attractor will transformed to the following Lorentz family is mode 1.

$$A_{11} = \begin{bmatrix} -10 & 10 & 0 \\ 28 & -1 & l_1 \\ 0 & -l_1 & -\frac{8}{3} \end{bmatrix}, \quad B_{11} = \begin{bmatrix} 1 & 0 & 0 \end{bmatrix}^T,$$

$$A_{21} = \begin{bmatrix} -10 & 10 & 0 \\ 28 & -1 & -l_2 \\ 0 & l_2 & -\frac{8}{3} \end{bmatrix}, \quad B_{21} = \begin{bmatrix} 1 & 0 & 0 \end{bmatrix}^T,$$
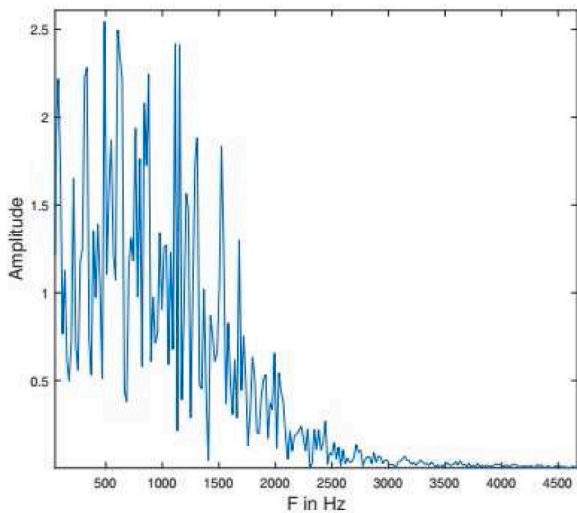
Fig. 11. The FFT measurement of the signal x_1 is based on the Discrete Fourier Transform (DFT). x-axis the frequency and the y-axis is the amplitude of the signal.
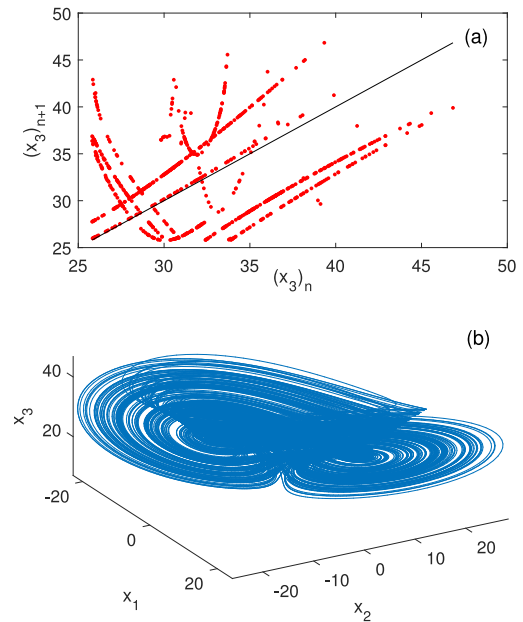

Fig. 12. (a) Poincar'e section in Chen attractor at $\alpha = 0.85$, $\rho = 28$ in the $(x_3)_n$ vs. $(x_3)_{n+1}$ plane and the corresponding (b) three-dimensional chaotic attractor.
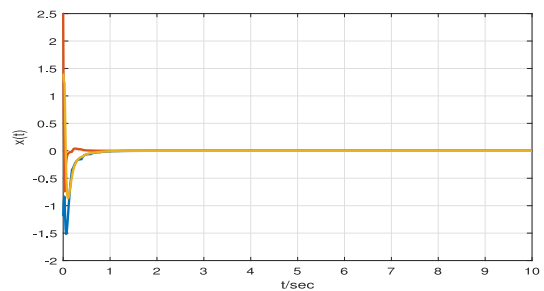
When $\delta = 1$, chaotic attractor will be transformed to the following Chen family is mode 2.

$$A_{12} = \begin{bmatrix} -35 & 35 & 0 \\ -7 & 28 & l_1 \\ 0 & -l_1 & -\frac{9}{3} \end{bmatrix}, \quad B_{12} = \begin{bmatrix} 1 & 0 & 0 \end{bmatrix}^T,$$

$$A_{22} = \begin{bmatrix} -35 & 35 & 0 \\ -7 & 28 & -l_2 \\ 0 & l_2 & -\frac{9}{3} \end{bmatrix}, \quad B_{22} = \begin{bmatrix} 1 & 0 & 0 \end{bmatrix}^T,$$

When $\delta = 0.8$, chaotic attractor will transform to the following Lu family is mode 3.

$$A_{13} = \begin{bmatrix} -(25*0.8+10) & 25*0.8+10 & 0 \\ 28-35*0.8 & 29*0.8-1 & l_1 \\ 0 & -l_1 & -\frac{8.8}{3} \end{bmatrix},$$

$$B_{13} = \begin{bmatrix} 1 & 0 & 0 \end{bmatrix}^T, \quad B_{23} = \begin{bmatrix} 1 & 0 & 0 \end{bmatrix}^T,$$

$$A_{23} = \begin{bmatrix} -(25*0.8+10) & 25*0.8+10 & 0 \\ 28-35*0.8 & 29*0.8-1 & l_2 \\ 0 & -l_2 & -\frac{8.8}{3} \end{bmatrix},$$

$$h_1(x_1(t)) = \frac{x_1(t)-l_1}{l_2-l_1}, \quad h_2(x_1(t)) = \frac{-x_1(t)+l_2}{l_2-l_1}.$$

The fuzzy SDC is as follows:

$$u(t) = \sum_{j=1}^{r} h_j(\varphi(x(t_k)))K_{jk}x(t_k), \quad t \in [t_k, t_{k+1}).$$

According to the above parameters and $\alpha = \beta = 0.1, \mu = 1$, sampling period $h_\mathcal{V} = 0.01$, $h_{\mathcal{U}} = 0.2$. By using LMIs in Theorem 2 and MATLAB LMI toolbox, then the average dwell time can be calculated as $\tau_a > 0.1543$ and the following gain matrices can be derived as follows.

$$K_{11} = \begin{bmatrix} 3.1924 & -1.0472 & 4.5453 \end{bmatrix}, K_{21} = \begin{bmatrix} 3.0236 & -1.0652 & 4.7434 \end{bmatrix},$$

$$K_{12} = \begin{bmatrix} 3.2638 & -1.0582 & 3.9556 \end{bmatrix}, K_{22} = \begin{bmatrix} 2.9238 & -1.0573 & 4.0334 \end{bmatrix},$$

$$K_{13} = \begin{bmatrix} 3.1531 & -1.0491 & 4.6462 \end{bmatrix}, K_{23} = \begin{bmatrix} 2.9537 & -1.0452 & 4.2434 \end{bmatrix}.$$

Based on the above control gains, the state and control responses of system (22) are given in Figs. 13 and 14, respectively.

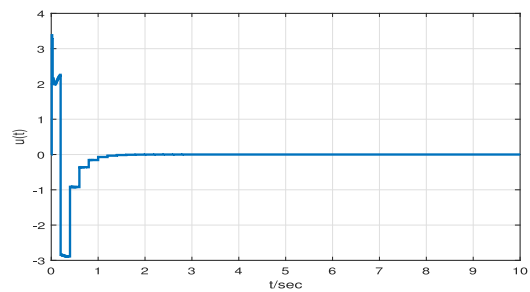**Fig. 13.** State responses for system (22) under the control gain matrices.

Fig. 14. Control responses of the system in Example 6.1.

7. Conclusions

In this article, based on the ADT technique, the switched chaotic system for fuzzy SDC has been examined. By utilizing the proper fuzzy LKF, novel inequality techniques and some sufficient conditions have been developed to obtain the exponential stability criteria for this type of chaotic system. Furthermore, the related SDC gains can be consolidated with the solvable LMIs within the maximum sampling interval. Simulation results are demonstrated such that the benefits of our theoretical techniques are validated. With these numerical results, it is inferred that the determined conditions have given less conservative results when contrasted with existing works and ready to accomplish

better stability achievement that has been exhibited the effectiveness of the proposed approach. Hence, in the future, the proposed techniques used in this paper will be adopted in the discrete-time case.

CRediT authorship contribution statement

R. Vadivel: Conceptualization, Methodology, Resources, Writing – review & editing. **S. Sabarathinam:** Formal analysis, Validation, Software. **Yongbao Wu:** Investigation, Formal analysis, Supervision, Writing – review & editing. **Kantapon Chaisena:** Formal analysis, Validation, Supervision. **Nallappan Gunasekaran:** Visualization, Methodology, Data curation, Writing – original draft.

Declaration of competing interest

The authors declare that they have no known competing financial interests or personal relationships that could have appeared to influence the work reported in this paper.

Data availability

No data was used for the research described in the article.

Appendix. Proof of Theorem 1

Proof. We realize that there are all things considered in the switching system during a sampling interval. Assuming that the system does not switch during any particular interval, the system modes and control gain are constantly coordinated. In the event that the system switches once during a sampling interval, before switching, the methods of system and control gain are coordinated, while subsequent switching can be different. Subsequently, we partition the interval into matched and mismatched to consider the stability.

Case 1: Consider the following LKF with matched intervals and $\sigma(t) = \kappa$:

$$V_\kappa(t) = \sum_{d=1}^{3} V_{\kappa d}(t), \ t \in [t_k, t_{k+1}), \tag{23}$$

where

$$
\begin{aligned}
V_{\kappa 1}(t) =& x^T(t) P_{1\kappa} x(t) + (t_{k+1} - t)[x(t) - x(t_k)]^T \\
& \times P_{2\kappa}[x(t) - x(t_k)],
\end{aligned}
$$

$$
V_{\kappa 2}(t) = (t_{k+1} - t) \begin{bmatrix} x(t) \\ x(t_k) \end{bmatrix}^T \overbrace{\coprod} \begin{bmatrix} x(t) \\ x(t_k) \end{bmatrix},
$$

$$
\begin{aligned}
V_{\kappa 3}(t) =& (t_{k+1} - t) \int_{t_k}^{t} e^{\alpha(s-t)} \dot{x}^T(s) Z_\kappa \dot{x}(s) ds \\
& - \frac{\pi^2}{4} \int_{t_k}^{t} e^{\alpha(s-t)} (x(s) - x(t_k))^T Z_\kappa (x(s) - x(t_k)) ds.
\end{aligned}
$$

and $\overbrace{\coprod} = \begin{bmatrix} \frac{1}{2}(\mathcal{X}_\kappa + \mathcal{X}_\kappa^T) & -\mathcal{X}_\kappa + \mathcal{Y}_\kappa, \\ * & -\mathcal{Y}_\kappa - \mathcal{Y}_\kappa^T + \frac{1}{2}(\mathcal{X}_\kappa + \mathcal{X}_\kappa^T) \end{bmatrix}$.

Taking the derivative of $V_\kappa(t)$, we get

$$
\begin{aligned}
\dot{V}_{\kappa 1}(t) =& \dot{x}^T(t) P_{1\kappa} x(t) + x^T(t) P_{1\kappa}^T \dot{x}(t) \\
& - [x(t) - x(t_k)]^T P_{2\kappa}[x(t) - x(t_k)] \\
& + (t_{k+1} - t)[x(t) - x(t_k)]^T P_{2\kappa} \dot{x}(t) \\
& + (t_{k+1} - t)\dot{x}^T(t) P_{2\kappa}^T[x(t) - x(t_k)] \\
& + \alpha x^T(t) P_{1\kappa} x(t) + \alpha(t_{k+1} - t)[x(t) \\
& - x(t_k)]^T P_{2\kappa}[x(t) - x(t_k)] - \alpha V_{\kappa 1}(t), \tag{24}
\end{aligned}
$$

$$
\begin{aligned}
\dot{V}_{\kappa 2}(t) =& -\alpha V_{\kappa 2}(t) - \begin{bmatrix} x(t) \\ x(t_k) \end{bmatrix}^T \overbrace{\coprod} \begin{bmatrix} x(t) \\ x(t_k) \end{bmatrix} \\
& + (t_{k+1} - t) \begin{bmatrix} \dot{x}(t) \\ 0 \end{bmatrix}^T \overbrace{\coprod} \begin{bmatrix} x(t) \\ x(t_k) \end{bmatrix}
\end{aligned}
$$

$$
\begin{aligned}
& + (t_{k+1} - t) \begin{bmatrix} x(t) \\ x(t_k) \end{bmatrix}^T \overbrace{\coprod} \begin{bmatrix} \dot{x}(t) \\ 0 \end{bmatrix} \\
& + \alpha(t_{k+1} - t) \begin{bmatrix} x(t) \\ x(t_k) \end{bmatrix}^T \overbrace{\coprod} \begin{bmatrix} x(t) \\ x(t_k) \end{bmatrix} \\
=& - \begin{bmatrix} x(t) \\ x(t_k) \end{bmatrix}^T \overbrace{\coprod} \begin{bmatrix} x(t) \\ x(t_k) \end{bmatrix} \\
& + \alpha(t_{k+1} - t) \begin{bmatrix} x(t) \\ x(t_k) \end{bmatrix}^T \overbrace{\coprod} \begin{bmatrix} x(t) \\ x(t_k) \end{bmatrix} \\
& + (t_{k+1} - t) \left[\dot{x}^T(t) \frac{\mathcal{X}_\kappa + \mathcal{X}_\kappa^T}{2} x(t) \right. \\
& + x^T(t) \left(\frac{\mathcal{X}_\kappa + \mathcal{X}_\kappa^T}{2} \right)^T \dot{x}(t) \bigg] \\
& + (t_{k+1} - t) \left[\dot{x}^T(t)(-\mathcal{X}_\kappa + \mathcal{Y}_\kappa) x(t_k) \right. \\
& + x^T(t_k) \left(-\mathcal{X}_\kappa + \mathcal{Y}_\kappa \right)^T \dot{x}(t) \bigg] - \alpha V_{\kappa 2}(t), \tag{25}
\end{aligned}
$$

$$
\begin{aligned}
\dot{V}_{\kappa 3}(t) =& (t_{k+1} - t)\dot{x}^T(t) Z_\kappa \dot{x}(t) - \int_{t_k}^{t} e^{\alpha(s-t)} \dot{x}^T(s) Z_\kappa \dot{x}(s) ds \\
& - \frac{\pi^2}{4}(x(t) - x(t_k))^T Z_\kappa (x(t) - x(t_k)) - \alpha V_{\kappa 3}(t). \tag{26}
\end{aligned}
$$

Now, we have

$$
- \int_{t_k}^{t} e^{\alpha(s-t)} \dot{x}^T(s) Z_\kappa \dot{x}(s) ds \leq - \int_{t_k}^{t} \dot{x}^T(s) Z_\kappa \dot{x}(s) ds. \tag{27}
$$

Then

$$
\begin{aligned}
& - \int_{t_k}^{t} \dot{x}^T(s) Z_\kappa \dot{x}(s) ds = \\
& - \int_{t_k}^{t} \dot{x}^T(s) \mathcal{Z}_\kappa \dot{x}(s) ds - \int_{t_k}^{t} \dot{x}^T(s) U_{33\kappa} \dot{x}(s) ds, \tag{28}
\end{aligned}
$$

where $\mathcal{Z}_\kappa = Z_\kappa - U_{33\kappa}$. Using the free-weighting matrix approach, we can get appropriately dimensioned matrix $\mathcal{M} = [\mathcal{M}_1, \mathcal{M}_2, \mathcal{M}_3]$ to make the following inequality hold:

$$
\int_{t_k}^{t} \begin{bmatrix} \zeta(t) \\ \dot{x}(s) \end{bmatrix}^T \begin{bmatrix} \mathcal{M}^T \mathcal{Z}_\kappa^{-1} \mathcal{M} & \mathcal{M}^T \\ * & \mathcal{Z}_\kappa \end{bmatrix} \begin{bmatrix} \zeta(t) \\ \dot{x}(s) \end{bmatrix} ds \geq 0, \tag{29}
$$

where $\zeta(t) = [x^T(t) \ \dot{x}^T(t) \ x^T(t_k)]^T$. This implies

$$
\begin{aligned}
& - \int_{t_k}^{t} \dot{x}^T(s) \mathcal{Z}_\kappa \dot{x}(s) ds \leq - \int_{t_k}^{t} \dot{x}^T(s) \mathcal{Z}_\kappa \dot{x}(s) ds \\
& + \int_{t_k}^{t} \begin{bmatrix} \zeta(t) \\ \dot{x}(s) \end{bmatrix}^T \begin{bmatrix} \mathcal{M}^T \mathcal{Z}_\kappa^{-1} \mathcal{M} & \mathcal{M}^T \\ * & \mathcal{Z}_\kappa \end{bmatrix} \begin{bmatrix} \zeta(t) \\ \dot{x}(s) \end{bmatrix} ds \\
=& (t - t_k) \zeta^T(t) \mathcal{M}^T \mathcal{Z}_\kappa^{-1} \mathcal{M} \zeta(t) \\
& + 2\zeta^T(t) \mathcal{M}^T [x(t) - x(t_k)]. \tag{30}
\end{aligned}
$$

Utilizing Leibniz–Newton formula, Lemma 1, and a fact $[U]_{3n\times 3n} \geq 0$, the following inequality is obtained: $[U]_{3n\times 3n} \geq 0$. Then, we obtain

$$
\begin{aligned}
& - \int_{t_k}^{t} \dot{x}^T(s) U_{33\kappa} \dot{x}(s) ds \leq - \int_{t_k}^{t} \begin{bmatrix} x^T(t) & x^T(t_k) & \dot{x}^T(s) \end{bmatrix} \\
& \times \begin{bmatrix} U_{11\kappa} & U_{12\kappa} & U_{13\kappa} \\ * & U_{22\kappa} & U_{23\kappa} \\ * & * & 0 \end{bmatrix} \begin{bmatrix} x(t) \\ x(t_k) \\ \dot{x}(s) \end{bmatrix} ds \\
=& x^T(t)[(t - t_k)U_{11\kappa} + U_{13\kappa} + U_{13\kappa}^T] x(t) \\
& + x^T(t)[(t - t_k)U_{12\kappa} - U_{13\kappa} + U_{23\kappa}^T] x(t_k) \\
& + x^T(t_k)[(t - t_k)U_{12\kappa}^T - U_{13\kappa}^T + U_{23\kappa}] x(t) \\
& + x^T(t_k)[(t - t_k)U_{22\kappa} - U_{23\kappa} - U_{23\kappa}^T] x(t_k). \tag{31}
\end{aligned}
$$

Then, we have

$$
\begin{aligned}
\dot{V}_{\kappa 3}(t) \leq &(t_{k+1}-t)\dot{x}^T(t)Z_\kappa \dot{x}(t) - \frac{\pi^2}{4}(x(t)-x(t_k))^T \\
&\times Z_\kappa(x(t)-x(t_k)) + (t-t_k)\zeta^T(t)\mathcal{M}^T \mathcal{Z}_\kappa^{-1}\mathcal{M}\zeta(t) \\
&+ 2\zeta^T(t)\mathcal{M}^T[x(t)-x(t_k)] + x^T(t)[(t-t_k)U_{11} \\
&+ U_{13}+U_{13}^T]x(t) + x^T(t)[(t-t_k)U_{12}-U_{13} \\
&+ U_{23}^T]x(t_k) + x^T(t_k)[(t-t_k)U_{12}^T - U_{13}^T + U_{23}]x(t) \\
&+ x^T(t_k)[(t-t_k)U_{22}-U_{23}-U_{23}^T]x(t_k) - \alpha V_{\kappa 3}(t).
\end{aligned}
\tag{32}
$$

For any properly dimensioned matrix $\mathcal{G}$, we get

$$
\begin{aligned}
0 =& 2[x^T(t)+\dot{x}^T(t)]\mathcal{G}[-\dot{x}(t)+\dot{x}(t)] \\
=& 2[x^T(t)+\dot{x}^T(t)]\mathcal{G}\Bigg[-\dot{x}(t)+h_i h_j\Big\{A_{i\kappa}x(t) \\
&+ (B_{i\kappa}K_{j\kappa})x(t_k)\Big\}\Bigg] \\
=& \sum_{i=1}^r \sum_{j=1}^r h_i(z(t))h_j(z(t_k))\Big\{-2x^T(t)\mathcal{G}\dot{x}(t) \\
&+ 2x^T(t)\mathcal{G}A_{i\kappa}x(t) + 2x^T(t)\mathcal{G}B_{i\kappa}K_{j\kappa}x(t_k) \\
&- 2\dot{x}^T(t)\mathcal{G}\dot{x}(t) + 2\dot{x}^T(t)\mathcal{G}A_{i\kappa}x(t) \\
&+ 2\dot{x}^T(t)\mathcal{G}B_i K_{j\kappa}x(t_k)\Big\}.
\end{aligned}
\tag{33}
$$

Then, substituting the left-hand side of (33) into $\dot{V}_\kappa(t)$, we have

$$
\begin{aligned}
\dot{V}_\kappa(t)+\alpha V_\kappa(t) \leq& \zeta^T(t)\Bigg[\Sigma^A+(t_{k+1}-t)\Sigma^B+(t-t_k)\Sigma^C \\
&+ (t-t_k)\mathcal{M}^T\mathcal{Z}_\kappa^{-1}\mathcal{M}\Bigg]\zeta(t).
\end{aligned}
\tag{34}
$$

Furthermore, by $h_k \in [h_\mathcal{V}, h_\mathcal{U}]$, we can express the following results:

$$
\begin{aligned}
\dot{V}_\kappa(t) \leq& -\alpha V_\kappa(t)+\zeta^T(t)\Bigg[\Sigma^A+\frac{t_{k+1}-t}{h_k}h_k\Sigma^B \\
&+ \frac{t-t_k}{h_k}h_k\big(\Sigma^C+\mathcal{M}^T\mathcal{Z}_\kappa^{-1}\mathcal{M}\big)\Bigg]\zeta(t) \\
=& -\alpha V_\kappa(t)+\zeta^T(t)\Bigg[\frac{t_{k+1}-t}{h_k}\Sigma^A+\frac{t-t_k}{h_k}\Sigma^A \\
&+ \frac{t_{k+1}-t}{h_k}h_k\Sigma^B+\frac{t-t_k}{h_k}h_k\big(\Sigma^C+\mathcal{M}^T\mathcal{Z}_\kappa^{-1}\mathcal{M}\big)\Bigg]\zeta(t) \\
=& -\alpha V_\kappa(t)+\zeta^T(t)\Bigg[\frac{t_{k+1}-t}{h_k}\big(\Sigma^A+h_k\Sigma^B\big) \\
&+ \frac{t-t_k}{h_k}\big(\Sigma^A+h_k\Sigma^C+h_k\mathcal{M}^T\mathcal{Z}_\kappa^{-1}\mathcal{M}\big)\Bigg]\zeta(t) \\
=& -\alpha V_\kappa(t)+\zeta^T(t)\Bigg[\frac{h_\mathcal{U}-h_k}{h_\mathcal{U}-h_\mathcal{V}}\big(\Sigma^A+h_k\Sigma^B\big) \\
&+ \frac{h_k-h_\mathcal{V}}{h_\mathcal{U}-h_\mathcal{V}}\big(\Sigma^A+h_\mathcal{U}\Sigma^B\big) \\
&+ \frac{h_\mathcal{V}-h_k}{h_\mathcal{U}-h_\mathcal{V}}\big(\Sigma^A+h_k\Sigma^C+h_k\mathcal{M}^T\mathcal{Z}_\kappa^{-1}\mathcal{M}\big) \\
&+ \frac{h_k-h_\mathcal{V}}{h_\mathcal{U}-h_\mathcal{V}}\big(\Sigma^A+h_k\Sigma^C+h_k\mathcal{M}^T\mathcal{Z}_\kappa^{-1}\mathcal{M}\big)\Bigg]\zeta(t).
\end{aligned}
\tag{35}
$$

According to the Schur complements, (10) implies

$$
\Sigma^A+h_k\Sigma^C+h_k\mathcal{M}^T\mathcal{Z}_\kappa^{-1}\mathcal{M} < 0,\ h_k \in \{h_\mathcal{V},\ h_\mathcal{U}\}.
\tag{36}
$$

From (35), we can obtain

$$
\dot{V}(t)+\alpha V_\kappa(t) < 0,\ t \in [t_k, t_{k+1}).
\tag{37}
$$

Case 2: Next, we consider the mismatched intervals and assume $t_s^\sigma \in [t_k, t_{k+1})$ with $t_s^{\sigma-}=\kappa$ and $t_s^\sigma=l \neq \kappa$. By following the identical approach as in Case 1, also (37) holds for $t \in [t_k, t_s^\sigma)$. Using the following LKF:

$$
V_{\kappa l}(t) = \sum_{d=1}^3 V_{\kappa l d}(t),
\tag{38}
$$

where

$$
\begin{aligned}
V_{\kappa l1}(t) =& x^T(t)P_{1\kappa l}x(t)+(t_{k+1}-t)[x(t)-x(t_k)]^T \\
&\times P_{2\kappa l}[x(t)-x(t_k)],
\end{aligned}
$$

$$
V_{\kappa 2}(t) = (t_{k+1}-t)\begin{bmatrix} x(t) \\ x(t_k) \end{bmatrix}^T \overbrace{\coprod_{\kappa l}} \begin{bmatrix} x(t) \\ x(t_k) \end{bmatrix},
$$

$$
\begin{aligned}
V_{\kappa l3}(t) =& (t_{k+1}-t)\int_{t_k}^t e^{\beta(s-t)}\dot{x}^T(s)Z_{\kappa l}\dot{x}(s)ds \\
&- \frac{\pi^2}{4}\int_{t_k}^t e^{\beta(s-t)}(x(s)-x(t_k))^T Z_{\kappa l}(x(s)-x(t_k))ds.
\end{aligned}
$$

$$
\overbrace{\coprod_{\kappa l}} = \begin{bmatrix} \frac{1}{2}(\mathcal{X}_{\kappa l}+\mathcal{X}_{\kappa l}^T) & -\mathcal{X}_{\kappa l}+\mathcal{Y}_{\kappa l}, \\ * & -\mathcal{Y}_{\kappa l}-\mathcal{Y}_{\kappa l}^T+\frac{1}{2}(\mathcal{X}_{\kappa l}+\mathcal{X}_{\kappa l}^T) \end{bmatrix}.
$$
Following the equivalent approach in Case 1, we get the inequality of (9) and (10):

$$
\dot{V}_{\kappa l}(t)+\beta V_{\kappa l}(t) < 0.
\tag{39}
$$

Moreover,

$$
V_{\kappa l}(t_s^\sigma) < V_{\kappa l}(t_s^{\sigma-}).
\tag{40}
$$

Utilizing (37), (39) and (40), the relationship between $V_{\kappa l}(t_{k+1}^-)$ and $V_{\kappa l}(t_k)$ can be characterized as

$$
V_{\kappa l}(t_{k+1}^-) \leq e^{(\alpha+\beta)h_k}e^{-\alpha(t_{k+1}-t_k)}V_{\kappa l}(t_k).
\tag{41}
$$

Under the condition (41), we have

$$
V_{\kappa l}(t_{k+1}) < \mu V_{\kappa l}(t_{k+1}^-).
\tag{42}
$$

Taking conditions (41), (42), and Definition 2 into examination, we get

$$
V_\kappa(t) \leq e^{((\alpha+\beta)h_\mathcal{U}+\ln\mu)N_0}.e^{(\frac{(\alpha+\beta)h_\mathcal{U}+\ln\mu}{\tau_a}-\alpha)(t-t_0)}V_{\sigma(t_0)}(t_0).
\tag{43}
$$

Defining $c = e^{((\alpha+\beta)h_\mathcal{U}+\ln\mu)N_0}$, and $\lambda = e^{\alpha-(\frac{(\alpha+\beta)h_\mathcal{U}+\ln\mu}{\tau_a})(t-t_0)} > 0$. Then

$$
V_{\sigma(t)}(t) < ce^{-\lambda(t-t_0)}V_{\sigma(t_0)}(t_0),
$$

From the LKF candidate, scalars ϕ and ϵ are satisfied with: $\epsilon\|x(t)\|^2 \leq V_{\sigma(t_0)}(t_0) \leq \phi e^{-\lambda(t-t_0)}\|x(t_0)\|_c^2$, which indicates

$$
\|x(t)\| \leq e^{-\frac{\lambda}{2}(t-t_0)}\sqrt{\frac{\phi}{\epsilon}}\|x(t_0)\|_c.
\tag{44}
$$

With the above analysis, we know that the closed-loop system (6) is exponentially stable. Hence, the complete proof. □

References

[1] Zadeh LA. Fuzzy logic. Computer 1988;21(4):83–93.

[2] Taniguchi T, Tanaka K, Ohtake H, Wang HO. Model construction, rule reduction, and robust compensation for generalized form of Takagi-Sugeno fuzzy systems. IEEE Trans Fuzzy Syst 2001;9(4):525–38.

[3] Wu G, Yang G-H, Wang H. ISS control synthesis of T–S fuzzy systems with multiple transmission channels under denial of service. J Franklin Inst B 2021;358(6):3010–32.

[4] Sun J, Zhang H, Wang Y, Sun S. Dissipativity analysis on switched uncertain nonlinear T–S fuzzy systems with stochastic perturbation and time delay. J Franklin Inst B 2020;357(18):13410–29.

[5] Park J, Kim J, Park D. LMI-based design of stabilizing fuzzy controllers for nonlinear systems described by Takagi-Sugeno fuzzy model. Fuzzy Sets and Systems 2001;122(1):73–82.

[6] Khaber F, Zehar K, Hamzaoui A. State feedback controller design via Takagi-Sugeno fuzzy model: LMI approach. Int J Comput Intell 2005;2(3):148–53.

[7] Lam H-K. LMI-based stability analysis for fuzzy-model-based control systems using artificial T–S fuzzy model. IEEE Trans Fuzzy Syst 2011;19(3):505–13.

[8] Nagamani G, Karthik C, Joo YH. Event-triggered observer-based sliding mode control for T-S fuzzy systems via improved relaxed-based integral inequality. J Franklin Inst B 2020;357(14):9543–67.

[9] Gunasekaran N, Joo YH. Robust sampled-data fuzzy control for nonlinear systems and its applications: Free-weight matrix method. IEEE Trans Fuzzy Syst 2019;27(11):2130–9.

[10] Gunasekaran N, Joo YH. Nie–Tan fuzzy method of fault-tolerant wind energy conversion systems via sampled-data control. IET Control Theory Appl 2020;14(11):1516–23.

[11] Ku C-C, Chang W-J, Tsai M-H, Lee Y-C. Observer-based proportional derivative fuzzy control for singular Takagi-Sugeno fuzzy systems. Inform Sci 2021;570:815–30.

[12] Shanmugam L, Joo YH. Stabilization of permanent magnet synchronous generator-based wind turbine system via fuzzy-based sampled-data control approach. Inform Sci 2021;559:270–85.

[13] Ding K, Zhu Q. Reliable intermittent extended dissipative control for uncertain fuzzy flexible spacecraft systems with Bernoulli stochastic distribution. IET Control Theory Appl 2021;15(7):911–25.

[14] Wang Y, Zou L, Ma L, Zhao Z, Guo J. A survey on control for Takagi-Sugeno fuzzy systems subject to engineering-oriented complexities. Syst Sci Control Eng 2021;9(1):334–49.

[15] Strogatz SH. Noninear dynamics and chaos: with applications to physics, biology, chemistry, and engineering. CRC Press; 2018.

[16] Rong CG, Xiaoning D. From chaos to order: methodologies, perspectives and applications, Vol. 24. World Scientific; 1998.

[17] Liu H, Wang X, Kadir A. Color image encryption using choquet fuzzy integral and hyper chaotic system. Optik-Int J Light Electron Opt 2013;124(18):3527–33.

[18] Rao R, Zhu Q. Exponential synchronization and stabilization of delayed feedback hyperchaotic financial system. Adv Difference Equ 2021;2021(1):1–13.

[19] Carroll TL, Pecora LM. Synchronizing chaotic systems. In: Chaos in communications, Vol. 2038. International Society for Optics and Photonics; 1993, p. 32–44.

[20] Park JH. Controlling chaotic systems via nonlinear feedback control. Chaos Solitons Fractals 2005;23(3):1049–54.

[21] Wang Y, Yu H. Fuzzy synchronization of chaotic systems via intermittent control. Chaos Solitons Fractals 2018;106:154–60.

[22] Zhang H. An integral sliding mode control of uncertain chaotic systems via disturbance observer. Complexity 2021;2021.

[23] Kumar S, Khan A. Controlling and synchronization of chaotic systems via Takagi–Sugeno fuzzy adaptive feedback control techniques. J ControlAutom Electr Syst 2021;1–11.

[24] Hu C, Jiang H, Teng Z. General impulsive control of chaotic systems based on a T–S fuzzy model. Fuzzy Sets and Systems 2011;174(1):66–82.

[25] Vadivel R, Joo YH. Reliable fuzzy H_∞ control for permanent magnet synchronous motor against stochastic actuator faults. IEEE Trans Syst Man Cybern Syst 2019.

[26] Gunasekaran N, Zhai G, Yu Q. Exponential sampled-data fuzzy stabilization of nonlinear systems and its application to basic buck converters. IET Control Theory Appl 2021;15(9):1157–68.

[27] Shanmugam L, Joo YH. Stability and stabilization for T–S fuzzy large-scale interconnected power system with wind farm via sampled-data control. IEEE Trans Syst Man Cybern Syst 2020;51(4):2134–44.

[28] Chen T, Francis B, Hagiwara T. Optimal sampled-data control systems. Proc IEEE 1998;86(4):741.

[29] Fridman E, Seuret A, Richard J-P. Robust sampled-data stabilization of linear systems: an input delay approach. Automatica 2004;40(8):1441–6.

[30] Ali MS, Gunasekaran N, Zhu Q. State estimation of T–S fuzzy delayed neural networks with Markovian jumping parameters using sampled-data control. Fuzzy Sets and Systems 2017;306:87–104.

[31] Gunasekaran N, Saravanakumar R, Syed Ali M, Zhu Q. Exponential sampled-data control for T–S fuzzy systems: application to Chua's circuit. Internat J Systems Sci 2019;50(16):2979–92.

[32] Wu Z-G, Shi P, Su H, Chu J. Sampled-data fuzzy control of chaotic systems based on a T-S fuzzy model. IEEE Trans Fuzzy Syst 2014;22(1):153–63.

[33] Lee TH, Lim CP, Nahavandi S, Park JH. Network-based synchronization of T-S fuzzy chaotic systems with asynchronous samplings. J Franklin Inst B 2018;355(13):5736–58.

[34] Liberzon D, Morse AS. Basic problems in stability and design of switched systems. IEEE Control Syst Mag 1999;19(5):59–70.

[35] Daafouz J, Riedinger P, Iung C. Stability analysis and control synthesis for switched systems: a switched Lyapunov function approach. IEEE Trans Automat Control 2002;47(11):1883–7.

[36] Hespanha JP, Morse AS. Stability of switched systems with average dwell-time. In: Proceedings of the 38th IEEE conference on decision and control (Cat. No. 99CH36304), Vol. 3. IEEE; 1999, p. 2655–60.

[37] Xiao H, Zhu Q. Stability analysis of switched stochastic delay system with unstable subsystems. Nonlinear Anal Hybrid Syst 2021;42:101075.

[38] Fu J, Li T-F, Chai T, Su C-Y. Sampled-data-based stabilization of switched linear neutral systems. Automatica 2016;72:92–9.

[39] Luo J, Li M, Liu X, Tian W, Zhong S, Shi K. Stabilization analysis for fuzzy systems with a switched sampled-data control. J Franklin Inst B 2020;357(1):39–58.

[40] Wang M, Qiu J, Chadli M, Wang M. A switched system approach to exponential stabilization of sampled-data T–S fuzzy systems with packet dropouts. IEEE Trans Cybern 2015;46(12):3145–56.

[41] Kuppusamy S, Joo YH. Nonfragile retarded sampled-data switched control of T–S fuzzy systems and its applications. IEEE Trans Fuzzy Syst 2019;28(10):2523–32.

[42] Liu H, Zhou G. Finite-time sampled-data control for switching T–S fuzzy systems. Neurocomputing 2015;166:294–300.

[43] Wang L, Lam H-K. New stability criterion for continuous-time Takagi-Sugeno fuzzy systems with time-varying delay. IEEE Trans Cybern 2018;49(4):1551–6.

[44] Lu R, Shi P, Su H, Wu Z-G, Lu J. Synchronization of general chaotic neural networks with nonuniform sampling and packet missing: a switched system approach. IEEE Trans Neural Netw Learn Syst 2018;29(3):523–33.

[45] Liu P-L. Improved delay-dependent robust stability criteria for recurrent neural networks with time-varying delays. ISA Trans 2013;52(1):30–5.

[46] Xia Y, Wang J, Meng B, Chen X. Further results on fuzzy sampled-data stabilization of chaotic nonlinear systems. Appl Math Comput 2020;379:125225.

[47] Zeng H-B, Teo KL, He Y, Wang W. Sampled-data stabilization of chaotic systems based on a T-S fuzzy model. Inform Sci 2019;483:262–72.